

ROLE OF LPA₃ IN MOUSE PLACENTAL DEVELOPMENT

by

ELIZABETH ANN DUDLEY

(Under the Direction of Xiaoqin Ye)

ABSTRACT

Lysophosphatidic acid (LPA) is a signaling molecule that acts through six G-protein coupled receptors, LPA₁₋₆. LPA₃-deficiency in mice was previously shown to cause delayed implantation, embryo crowding, and placental hypertrophy that were only associated with maternal genotype and not fetal genotypes. It was hypothesized that *Lpar3*-deficiency alters placentation which may lead to placental hypertrophy. Realtime PCR, for temporal expression of *Lpar3* in placenta; *in situ* hybridization, for localization of *Lpar3* in D13.5 placenta; and histology of D13.5 placentas were conducted. These data demonstrated spatiotemporal expression of *Lpar3* mRNA in the mouse placenta and a critical role of maternal LPA₃ in the mouse placental development. Additionally, it was hypothesized that LPA₃-mediated signaling may promote uterine stromal cell proliferation to prepare the uterus for embryo implantation via ERK phosphorylation. Preliminary data indicate that the total ERK is not altered in the preimplantation D3.5 *Lpar3*-deficient uterus.

INDEX WORDS: LPA, LPA₃, *Lpar3*^{-/-} mice, placenta, uterus, ERK

ROLE OF LPA₃ IN MOUSE PLACENTAL DEVELOPMENT

by

ELIZABETH ANN DUDLEY

BS, CREIGHTON UNIVERSITY, OMAHA, NE, 2011

A Thesis Submitted to the Graduate Faculty of The University of Georgia in Partial
Fulfillment of the Requirements for the Degree

MASTER OF SCIENCE

ATHENS, GEORGIA

2015

© 2015

ELIZABETH ANN DUDLEY

All Rights Reserved

ROLE OF LPA₃ IN MOUSE PLACENTAL DEVELOPMENT

by

ELIZABETH ANN DUDLEY

Major Professor: Xiaoqin Ye

Committee: Mary Alice Smith
Shelley Hooks

Electronic Version Approved:

Suzanne Barbour
Dean of the Graduate School
The University of Georgia
December 2015

ACKNOWLEDGEMENTS

Dr. Xiaoqin Ye

Committee members:

Dr. Mary Alice Smith

Dr. Shelley Hooks

Dr. Tamas Nagy

Current lab members:

Rong Li

Ahmed El Zowalaty

Zidao Wang

Administrative support from:

Joanne Mauro

Kali King

Misty Patterson

Financial support from:

NIH

Department of Physiology and Pharmacology

Interdisciplinary Toxicology Program

TABLE OF CONTENTS

	Page
ACKNOWLEDGEMENTS	iv
LIST OF ABBREVIATIONS.....	vii
LIST OF FIGURES AND TABLE	viii
CHAPTER	
1 INTRODUCTION and LITERATURE REVIEW	1
1.1 LPA signaling.....	1
1.2 LPA ₃ signaling during pregnancy	4
1.3 Placentation	7
1.4 Hypotheses and specific aim	11
2 ROLE of LPA ₃ in MOUSE PLACENTAL DEVELOPMENT.....	12
2.1 Abstract.....	13
2.2 Introduction and Literature Review	13
2.3 Materials and Methods.....	15
2.4 Results.....	18
2.5 Discussion	23
3 ERK EXPRESSION in <i>Lpar3</i> ^{-/-} MOUSE UTERUS during EMBRYO IMPLANTATION.....	27
3.1 Abstract.....	28
3.2 Introduction and Literature Review	29

3.3 Materials and Methods.....	30
3.4 Results.....	32
3.5 Discussion	34
4 COLLABORATIVE WORK	37
5 CONCLUSION	42
REFERENCES.....	44

LIST OF ABBREVIATIONS

ATX	autotaxin
C-TGC	canal trophoblast cell
D (E)	gestation (embryonic) day
DGK	diacylglycerol kinase
GlyT	glycogen trophoblast
GPCR	G protein-coupled receptor
Het	Heterozygous
ERK	extracellular signal-regulated kinases
ISH	<i>in situ</i> hybridization
KO (hom)	LPA ₃ knockout
LCAT	lecithin-cholesterol acyltransferase
LE	luminal epithelium
LPA	lysophosphatidic acid
LPA ₃	lysophosphatidic acid receptor 3
LPL	lysophospholipid
MAPK	mitogen-activated protein kinase
PLA	phospholipase A
P-TGC	parietal trophoblast giant cell
S-TGC	sinusoidal trophoblast cell
SpA-TGC	spiral artery trophoblast cell
SpT	spongiotrophoblast
WT	wild type

LIST OF FIGURES

Figure 1.1 LPA production	2
Figure 1.2 LPA signaling pathways	3
Figure 1.3 Mouse placental development	7
Figure 1.4 Definitive chorioallantoic placenta	8
Figure 1.5 Interhemal membrane	9
Figure 1.6 Maternal and fetal circulation in placenta	10
Figure 2.1 Realtime PCR protocol	16
Figure 2.2 <i>In situ</i> hybridization protocol	17
Figure 2.3 Genotyping using PCR	18
Figure 2.4 Dissection of placenta	18
Figure 2.5 Quantification of mRNA expression in WT placentas by realtime PCR	19
Figure 2.6 <i>Lif</i> and <i>Lpar3</i> <i>in situ</i> hybridization	20
Figure 2.7 <i>Tpm1</i> and <i>Lpar3</i> <i>in situ</i> hybridization	21
Figure 2.8 Histology of WT (A,C,E) and <i>Lpar3</i> ^{-/-} (B,D,F) D13.5 placentas	22
Figure 2.9 Histology of D13.5 placentas	23
Figure 3.1 Tissue collection	32
Figure 3.2 Protein Standard	33
Figure 3.3 Western blot of pERK and tERK	33
Figure 3.4 Immunohistochemistry of tERK and pERK	34

Figure 4.1 Pilot western blot using a customized anti-Seipin antibody in adult mouse tissues	38
Figure 4.2 Immunohistochemistry detection of pER α and ER α in control and Lpar3 ^{-/-} uteri during embryo implantation	39
Figure 4.3 Male fertility test and detection of LHFPL2 in uterus	40
Figure 4.4 Pilot western blot for vimentin and E-cadherin in D0.5 and D3.5 uteri	41

TABLE

Table 1. Primers used in the study	26
--	----

CHAPTER 1

INTRODUCTION and LITERATURE REVIEW

This thesis focuses on LPA₃-mediated signaling in placentation using *Lpar3*^{-/-} mouse model. In Chapter 1 we review three main aspects related to this focus of the thesis: LPA signaling, LPA₃ signaling during pregnancy, and placentation, and states the hypothesis and specific aim of the study.

1.1 LPA signaling

1.1.1 Overview

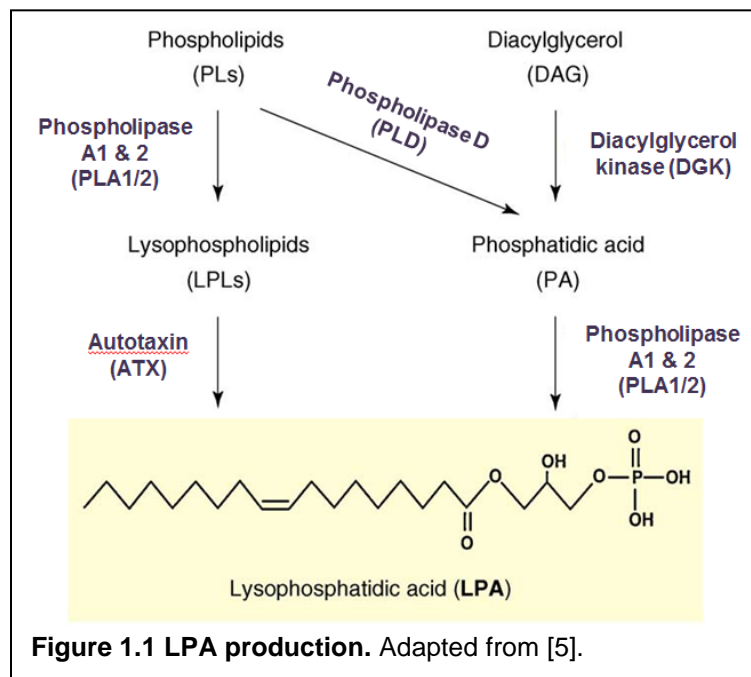
Lysophosphatidic acid (LPA) is a simple phospholipid that is involved in many physiological pathways. LPA is found in biological fluids including serum, plasma, and tears and can be produced in various cell types [3, 4]. The exact mechanisms of LPA metabolism remain elusive, but two pathways of LPA production have been reported. These pathways will be reported in Section 1.1.2 LPA production. Extracellular LPA is stabilized and transported by binding to proteins such as albumin and fatty acid binding protein [5]. LPA activates six known G protein-coupled receptors (GPCRs) in mammals [6, 7]. These receptors are identified in Section 1.1.3 LPA Receptors.

1.1.2 LPA production

The first pathway of LPA production mainly occurs in extracellular fluid such as serum and plasma, and the second pathway is involved in cellular LPA synthesis [3]. In the first pathway, LPA is produced from phospholipids (Fig 1.1). Phospholipase A₁

(PLA₁), PLA₂, or lecithin-cholesterol acyltransferase (LCAT) removes one acyl group from the phospholipid to form a lysophospholipid (LPL). LPLs are then converted into LPA by autotaxin (ATX), a plasma enzyme that has lysophospholipase D activity [8]. In addition to producing LPA in the blood, ATX has been reported to be active in this pathway in follicular fluid, embryonic blood vessel formation, and in trophoblast cells in human placenta [9].

In the second pathway, phosphatidic acid is produced by either phospholipase D acting on phospholipids or diacylglycerol kinase (DGK) phosphorylating diacylglycerol (Fig 1.1). The phosphatidic acid is then hydrolyzed by either PLA₁ or PLA₂ [8].



1.1.3 LPA receptors

LPA is a ligand for six known seven-transmembrane G protein-coupled receptors, LPA₁-LPA₆ [6, 7]. The human genes are designated *LPAR1-6*, and the mouse genes are designated *Lpar1-6* [7]. They have tissue-specific receptor expression patterns [3, 6]. For example, *Lpar1-3* but not *Lpar4-5* have significant expression levels

in mouse uterus and testis [6, 10-12]. In addition to having differential expression in tissues, LPA receptors have preferences for ligand structures. While LPA₁ and LPA₂ do not have a preference for 1-acyl-LPA or 2-acyl-LPA, LPA₃ has a high affinity for the 2-acyl-LPA structure [5]. These differences in LPA receptor expression and activity lead to the different roles that the receptors have in LPA signaling.

1.1.4 LPA signaling

LPA receptors couple with multiple G proteins to activate a variety of downstream signaling pathways (Fig 1.2). LPA₁, the first identified LPA receptor, activates three G proteins: G_{12/13}, G_q, and G_i. G_{12/13} activates signaling through the Rho-ROCK and Rho-SRF pathways. LPA₃ also couples with G_q and G_i. G_q activates the phospholipase C (PLC) pathways which induces calcium ion mobilization through IP₃ and protein kinase C through DAG. G_i activates the PLC pathways but also promotes LPA-induced activation of mitogen-activated protein kinase (MAPK, also known as ERK) [6].

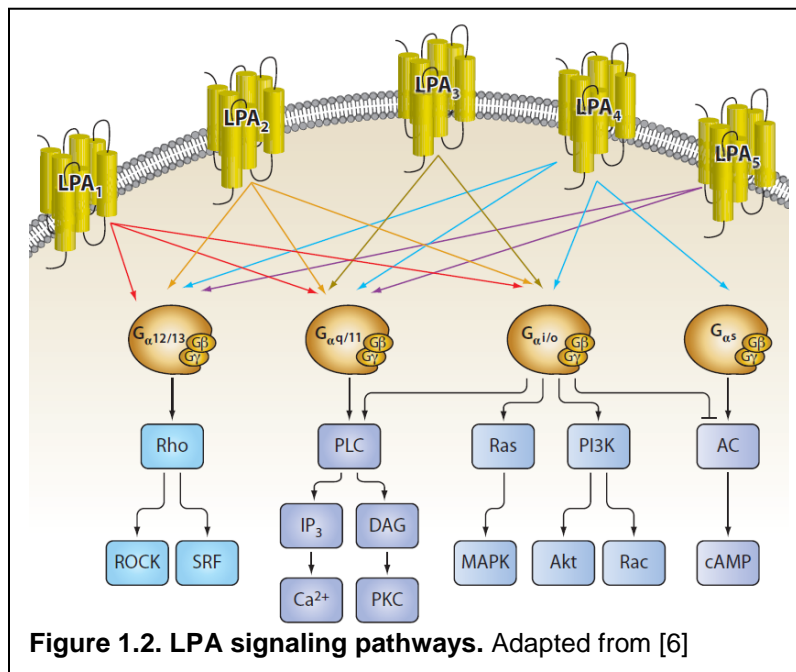


Figure 1.2. LPA signaling pathways. Adapted from [6]

1.2 LPA₃ signaling during pregnancy

1.2.1 Overview

LPA₃ is differentially expressed during pregnancy. *Lpar3* has much higher expression during the periimplantation period in murine, porcine, and ovine uterus [3, 5]. LPA produced in human placental trophoblasts may be involved in controlling trophoblast proliferation and differentiation and placental vascular remodeling, but the receptors through which it signals are not understood [3].

1.2.2 Embryo implantation

LPA₃ is highly expressed during the periimplantation period in multiple animal models. In sheep, LPA₃ has been detected in the luminal and glandular epithelium in the uterus and in the trophectoderm of the embryo, suggesting a role for LPA signaling in embryo elongation and implantation [3]. Similarly in pigs, *Lpar3* expression peaks when the embryo elongates prior to implantation and is found in the luminal and glandular epithelium [5].

In mice, *Lpar3* expression peaked on gestation day 3.5 (D3.5) and was found in the luminal epithelium (LE) of the uterus [10]. *Lpar3* is the only LPA receptor that is highly upregulated during the periimplantation period, and it is localized to the LE which is the first layer of cells the blastocyst communicates with during implantation. Thus, LPA₃ is likely involved in the establishment of uterine receptivity to the implanting embryos [13]. Deletion of *Lpar3* resulted in delayed implantation and embryo crowding [10]. Implantation sites, detected by Evans blue dye labeling, are seen in the uterus on D4.5 in control mice but not in *Lpar3*-deficient mice. Instead, the *Lpar3*-deficient mice have detectable implantation sites on D5.5 (mating night as D0). The *Lpar3*-deficient

mice also had a reduced number of implantation sites compared to the control mice. Comparable numbers of pre-implantation blastocysts were found in control (on D3.5) and *Lpar3*-deficient (on D4.5) uteri, suggesting that the implantation delay was not caused by embryonic LPA signaling.

Lpar3-deficient blastocysts that were transferred to control mice did not exhibit implantation or spacing problems. These results indicate that maternal, not embryonic, LPA₃ signaling is responsible for the altered implantation. The embryos that did implant in *Lpar3*-deficient mice were clustered in the uterus proximal to the cervix [10]. *Lpar3*-deficient uteri lacked the LPA₃-specific agonist-induced rapid uterine contraction seen in WT uteri prior to embryo implantation [14]. This contraction is important for appropriate embryo spacing, so the lack of uterine contraction may account for the embryo crowding seen in *Lpar3*-deficient mice [10].

Recent evidence demonstrates that delayed embryo implantation and embryo crowding in *Lpar3*-deficient mice are two segregated events. First, when a single WT embryo was transferred into pseudopregnant WT or *Lpar3*-deficient mice on D2.5, on-time implantation was detected in WT mice but not *Lpar3*-deficient mice on D4.5, indicating that embryo crowding is not a cause for delayed embryo implantation in *Lpar3*-deficient mice [14]. Second, when delayed implantation was rescued by prostaglandin agonists [10, 15], or RU486 or 17 β -estradiol [16], embryo crowding persisted in *Lpar3*-deficient mice [10, 15, 16].

1.2.3 Pregnancy

In addition to embryo crowding and delayed implantation, *Lpar3*-deficient mice also produced smaller litters with longer gestation periods. The embryo crowding

caused further problems later in gestation. Two or more embryos often shared a single placenta or two partially conjoined placentas. These placentas exhibited hypertrophy. *Lpar3*-deficient mice had an increased incidence of embryonic death as the pregnancy progressed leading to the decreased litter size. The viable embryos from *Lpar3*-deficient mice were smaller than those from control mice, but the *Lpar3*-deficient newborns were heavier, possible due to the longer pregnancy and smaller litter size [10]. *Lpar3* is expressed in the mouse placenta, but its localization and role in placental development and function are not yet known.

During human pregnancy, there is progressively increased production of LPA by lysophospholipase D in maternal blood [17]. Serum autotaxin (ATX) levels also increase with the progression of human pregnancy. ATX is a key enzyme for LPA production (Fig. 1.1). However, the serum ATX levels are significantly decreased in patients with pregnancy-induced hypertension compared to those with normal pregnancy in the third trimester [18]. Interestingly, the placental ATX expression correlates with serum ATX levels during pregnancy [19]. A recent study shows decreased placental ATX expression in patients with early-onset preeclampsia [20]. One study indicates that *LPAR3* is expressed at high levels in placentas from patients with mild and severe preeclampsia [21]. The significance of altered LPA production and *LPAR3* expression during pregnancy with or without preeclampsia remains unknown.

1.2.4 Regulation of *Lpar3*

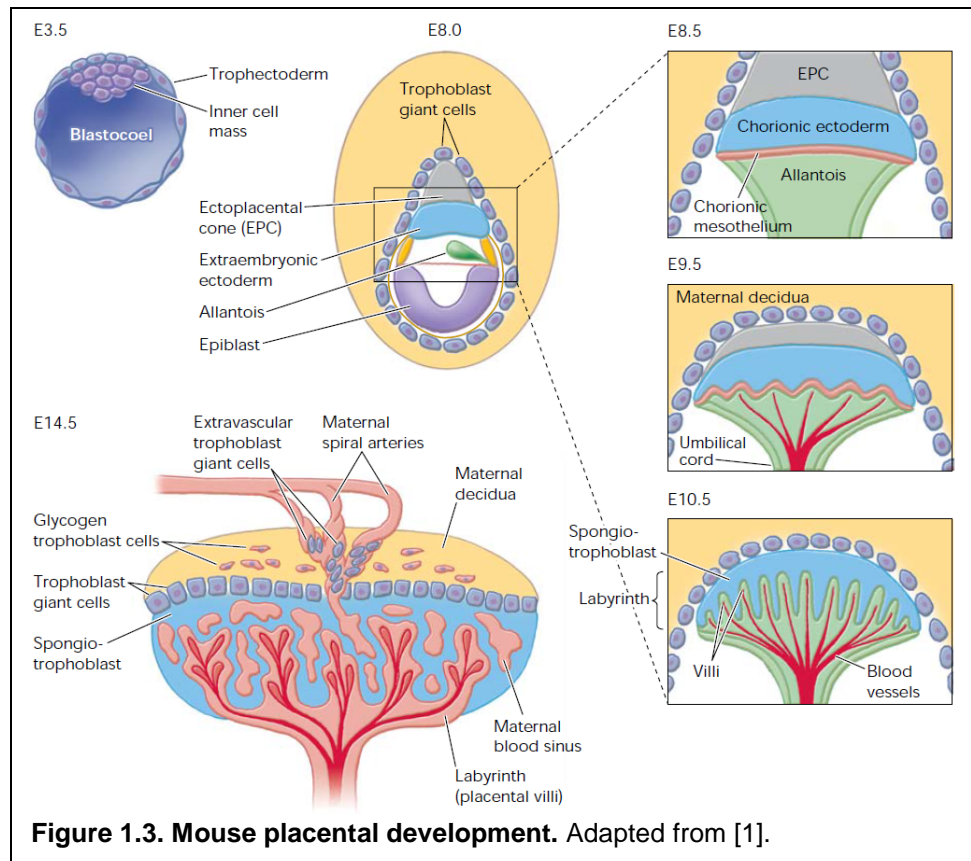
Lpar3 expression is regulated by progesterone and 17 β -estradiol (E₂) [12]. After hormone treatment and real-time PCR, it was determined that progesterone caused increased expression of *Lpar3* and E₂ caused decreased expression of *Lpar3* in the

ovariectomized mouse uterus. The progesterone-induced upregulation could be prevented by treatment with RU486, a progesterone receptor antagonist. These data suggest that progesterone receptor is involved in regulation of *Lpar3*.

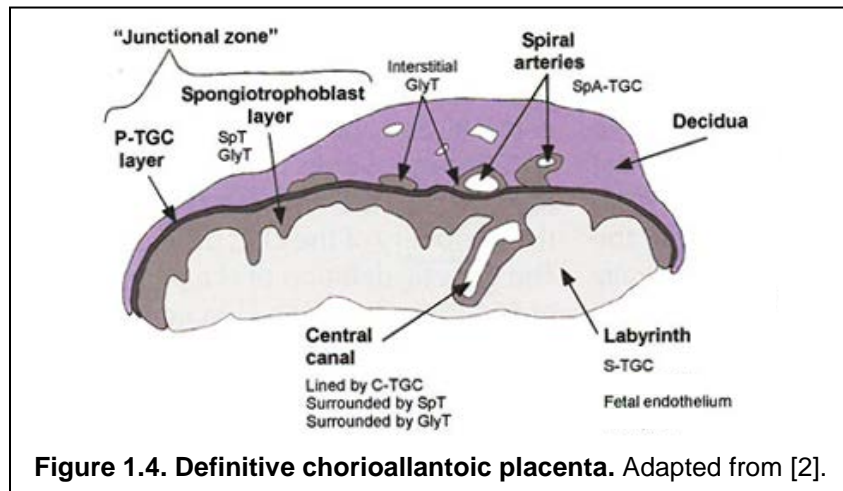
1.3 Placentation

1.3.1 Overview

Mice have a definitive chorioallantoic placenta. The extraembryonic lineages, from which the placenta develops, originate from the trophoblasts in embryonic day (E) 3.5 blastocysts prior to the initiation of embryo implantation in E4.0 (Fig. 1.3) [1]. Chorioallantoic attachment occurs at E8.0. Labyrinth forms by E10.5. The mouse placenta matures by E14.5 (Fig. 1.3) [1].



Structurally, the placenta has four distinct layers: the labyrinth, spongiotrophoblast layer, parietal trophoblast giant cell (P-TGC) layer, and the maternal decidua. The labyrinth is closest to the fetus and is the largest layer of the placenta where nutrient, waste, and gas exchange between the maternal and fetal blood occurs. The spongiotrophoblast layer is made of spongiotrophoblast (SpT) and glycogen trophoblast (GlyT) cells and has significant endocrine activity. The P-TGC layer is made of large but thin, invasive, polyploid cells which mediate invasion into the uterine endometrium. The spongiotrophoblast and P-TGC layers make up the “junctional zone” (Fig. 1.4). The maternal decidua is mainly decidual (endometrial stromal) cells but also includes uterine natural killer cells, invading trophoblast cells, and maternal vasculature [2].



1.3.2 Chorioallantoic attachment

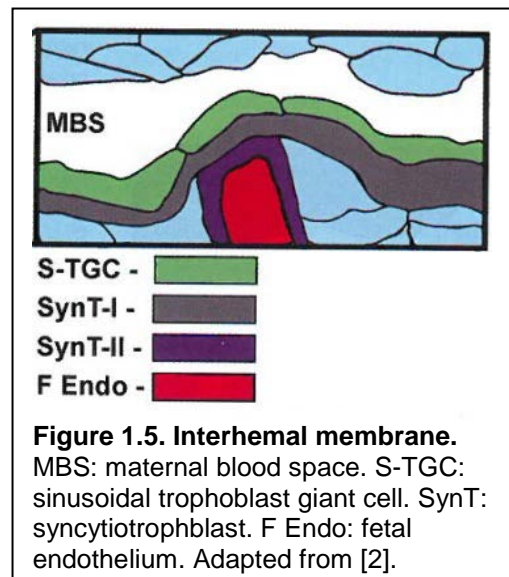
The development of the chorioallantoic placenta begins in mice around D7.0 with the protrusion of the extraembryonic ectoderm and mesoderm into the proamniotic cavity. Further proliferation of these cells separates the single proamniotic cavity into three distinct cavities: the amniotic cavity, lined with epiblast cells; the exocoelomic

cavity, lined with embryonic mesoderm cells; and the ectoplacental cone cavity, lined with extraembryonic ectoderm. The layer separating the exocoelomic and ectoplacental cone cavities is the chorion. During D7, the allantois buds from the mesoderm in the exocoelomic cavity and extends through the cavity to later attach to the chorion (around D8.5) (Fig. 1.3) [1, 2].

On D8, the chorion continues to proliferate and contacts with the lining of the ectoplacental cone cavity, causing adhesion between the two layers and occlusion of the cavity. Soon after, the allantois that had grown through the exocoelomic cavity attaches to the chorion, a process referred to as chorioallantoic attachment. At the chorioallantoic interface, the allantois is involved in vascularizing the developing placental labyrinth. The placental vasculature will be linked to the yolk sac and fetal blood system through the allantois, which is continuous with the primitive streak [2].

1.3.3 Labyrinth development

After chorioallantoic attachment, chorionic trophoblast cells differentiate into distinct cell layers which will form the interhemal membrane separating the maternal and fetal blood spaces in the labyrinth (Fig 1.5). The maternal blood spaces are lined with sinusoidal trophoblast giant cells (S-TGCs). Two layers of syncytiotrophoblast cell layers, multinucleated cell layers created by fusion



of cytotrophoblast cells, lie under the S-TGC layer. The cells lining the fetal blood spaces are fetal endothelial cells. These layers are present by D9.5 but undergo further

involution and branching to increase the surface area of the fetal vasculature. Additionally, these layers thin continually throughout gestation to increase the efficiency of exchange between the maternal and fetal blood spaces. By D12.5 the S-TGCs become perforated to allow direct contact between maternal blood and the first syncytiotrophoblast layer [2].

1.3.4 Junctional zone development

Cells in the ectoplacental cone differentiate into a variety of cells which will populate the junctional zone. P-TGCs form a layer adjacent to the maternal decidua. SpT and GlyT cells make up the bulk of the SpT layer and support the proper development of the labyrinth. Two additional subtypes of trophoblast giant cells (besides P-TGCs and S-TGCs) develop to line the maternal vasculature in the SpT layer, namely the spiral arteries (SpA-TGCs) and the canals (C-TGCs) [2].

1.3.5 Maternal and fetal circulation

Maternal spiral arteries in the SpT layer converge into several large canals which carry the blood into the labyrinth. The blood enters the maternal blood spaces, or sinusoids, which are lined with S-TGCs of the interhemal membrane (Fig. 1.5). The maternal blood moves through the sinusoids back to the SpT layer [22]. Fetal blood vessels develop from the allantois through vasculogenesis. After chorioallantoic attachment, primary villi and the developing blood vessels grow

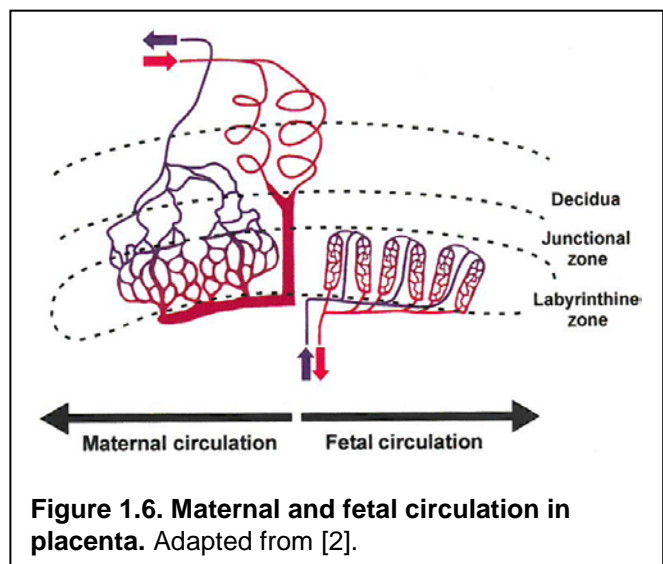


Figure 1.6. Maternal and fetal circulation in placenta. Adapted from [2].

into the chorion and begin branching. The mechanism and signaling interactions between allantois and the chorion which result in villous development are not fully understood [1]. Once developed, fetal arterioles carry fetal blood toward the junctional zone before branching into capillaries that move the blood back toward the fetus. Ultimately, the maternal and fetal vasculatures form a counter-current exchange in the labyrinth to efficiently transport the necessary nutrients, waste, and gases (Fig. 1.6) [2].

The definitive placenta (maternal decidua, junctional zone, and labyrinth) is fully functional by D12.5 but continues to grow with expansion and loss of various cell types through gestation. Less is known about the development of the placenta after D14.5 than the formation of the definitive placenta by D12.5 [2].

1.4 Hypothesis and specific aim

In Chapter 2 we hypothesize that deletion of *Lpar3* alters placentation which may lead to placental hypertrophy that could contribute to decreased embryo weight, increased post-implantation embryonic death, and reduced litter size in *Lpar3*^{-/-} females. The specific aim is to determine *Lpar3* mRNA expression in the mouse placenta throughout placenta development using realtime PCR and on D13.5 using *in situ* hybridization in an *Lpar3*-deficient (*Lpar3*^{-/-}) mouse model. We will determine alterations to placental structure by analyzing placenta histology on D13.5. In Chapter 3 we hypothesize that LPA₃-mediated signaling may promote uterine stromal cell proliferation to prepare the uterus for embryo implantation via ERK phosphorylation. We will analyze ERK and phosphorylated-ERK protein using western blotting and immunohistochemistry in D3.5 mouse uterus in the same *Lpar3*^{-/-} mouse model.

CHAPTER 2

ROLE of LPA₃ in MOUSE PLACENTAL DEVELOPMENT¹

¹ Dudley, EA; Li, R; El Zowalaty, AE; Wang, Z; and Ye, X. To be submitted to Biology of Reproduction

2.1 Abstract

Lysophosphatidic acid (LPA) is a signaling molecule that acts through six G-protein coupled receptors, LPA₁₋₆. LPA₃-deficiency in mice was previously shown to cause delayed implantation, embryo crowding, and placental hypertrophy that were only associated with maternal genotype and not fetal genotypes. It is hypothesized that *Lpar3*-deficiency alters placentation which may lead to placental hypertrophy. Realtime PCR revealed upregulation of *Lpar3* mRNA from D9.5 placenta to D13.5 placenta. *In situ* hybridization on D13.5 placenta has not been successful. Histology of D13.5 placentas showed that singleton or conjoined placentas from *Lpar3*^{-/-} females had similar abnormalities, including a very dense spongiotrophoblast layer with reduced numbers of vascular channels compared to WT control. These data demonstrated spatiotemporal expression of *Lpar3* mRNA in the mouse placenta and a critical role of maternal LPA₃ in the mouse placental development.

2.2 Introduction and Literature Review

Lysophosphatidic acid (LPA) is a simple phospholipid that is involved in many physiological pathways. LPA is found in many biological fluids including serum, plasma, and tears and can be produced in various cell types [3, 4]. LPA is a ligand for six GPCRs, LPA₁-LPA₆ [3, 6]. In humans, *LPAR3* is expressed at high levels in placentas from patients with gestational hypertension and preeclampsia, although its cellular localization is unknown. *Lpar3*, the gene for LPA₃ in mice, has been detected in the oviduct, placenta, and uterus of the female reproductive system [10]. LPA₃ is involved in

uterine smooth muscle contraction which may influence both embryo spacing at the beginning of pregnancy and parturition at the end of the pregnancy [5].

LPA₃ is highly expressed during the periimplantation period in multiple animal models. In sheep, LPA₃ has been detected in the luminal and glandular epithelium in the uterus and in the trophoctoderm of the embryo, suggesting a role for LPA signaling in embryo elongation and implantation [3, 23]. Similarly in pigs, *Lpar3* expression peaks when the embryo elongates prior to implantation and is found in the luminal and glandular epithelium [5].

In mice, *Lpar3* expression peaked on embryonic/gestation day 3.5 (E3.5 or D3.5) and was mainly found in the luminal epithelium (LE) of the uterus. Deletion of *Lpar3* in mice (*Lpar3*^{-/-}) leads to delayed uterine receptivity for embryo implantation, embryo crowding, increased post-implantation embryonic death, and reduced litter size. These phenotypes are unrelated to the genotypes of the mating males, indicating maternal defects [10]. In addition to and possibly as a result of embryo crowding and delayed implantation, *Lpar3*^{-/-} mice also produced smaller litters with longer pregnancies. The embryo crowding caused further problems later in gestation. Two or more embryos often shared a single placenta or two partially conjoined placentas. These placentas exhibited hypertrophy [10].

Both embryo implantation timing and embryo spacing can affect litter size. However, restoration of on-time implantation and partial alleviation of embryo crowding using pharmacological approaches cannot fully restore the litter size from *Lpar3*^{-/-} females to that from wild type (WT) females [10, 15]. The gestation day 18.5 (D18.5) placentas from *Lpar3*^{-/-} females are heavier than those from WT females. Conjoined

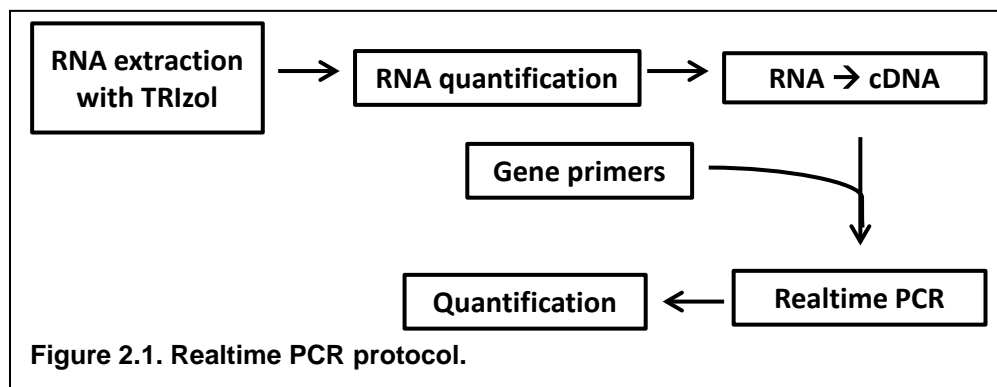
placentas from *Lpar3*^{-/-} females are often observed due to embryo crowding from defective implantation. However, the weights of embryos up to D18.5 from *Lpar3*^{-/-} females are significantly lower than those from WT females [10]. Delayed embryo implantation is a known cause for the reduced embryo weight. The lower embryo weight may also be caused by placental defects in the *Lpar3*^{-/-} females. We hypothesize that deletion of *Lpar3* alters placentation which may lead to placental hypertrophy that could contribute to decreased embryo weight, increased post-implantation embryonic death, and reduced litter size in *Lpar3*^{-/-} females. To test this hypothesis, the expression of *Lpar3* mRNA in the mouse placenta was determined throughout placental development using realtime PCR and on D13.5 using *in situ* hybridization. We also analyzed histology of D13.5 *Lpar3*^{-/-} placentas.

2.3 Materials and Methods

Animals. Wild type (WT), *Lpar3* heterozygous (*Lpar3*^{+/-} / Het), and *Lpar3*^{-/-} (hom) mice in a mixed background (129/SvJ and C57BL/6) were generated from a colony at the University of Georgia which was originally derived at The Scripps Research Institute. The mice were housed in polypropylene cages with free access to food and water from water sip tubes with a reverse-osmosis system. The animal facility has 12 hour light:dark days with 30%-50% relative humidity at 23±1°C. All methods used in this study were approved by the University of Georgia Institutional Animal Care and Use Committee and conform to National Institutes of Health guidelines and public law. Females were naturally mated with males. The day a plug was found was designated D0.5.

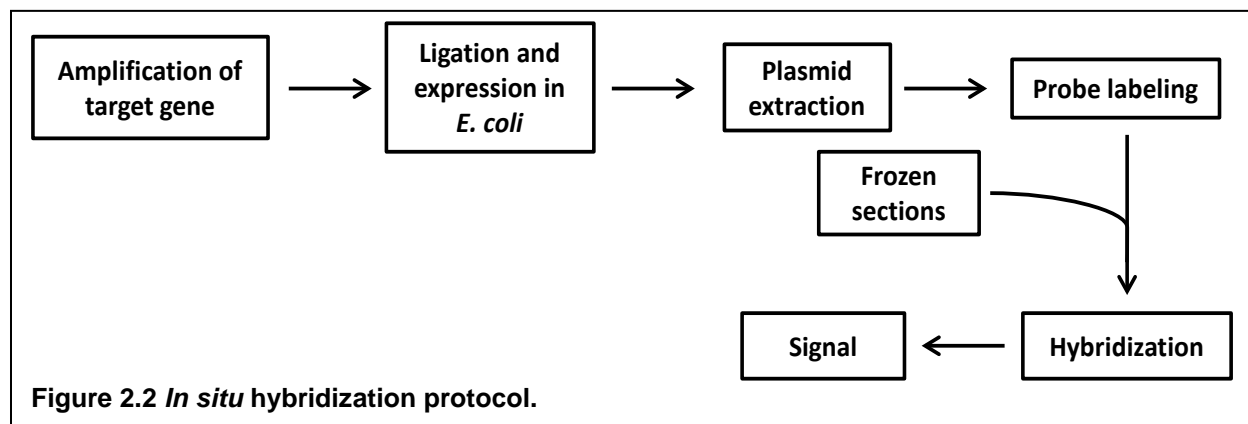
Genotyping and tissue collection. Mice were dissected at various time points, and placentas were collected and either fixed in formalin or flash frozen on dry ice and stored at -80°C. Fetal tissue was collected for genotyping the fetal side of the placenta. Genotyping was done using primers listed in Table 1.

RNA isolation and realtime PCR. Flash frozen placentas (D9.5, D11.5, D13.5, D15.5, and D18.5, N=3) from WT females mated with WT males were used for RNA isolation using TRIzol reagent (Invitrogen, Carlsbad, CA, USA). The isolation was performed following manufacturer's instructions except each sample was extracted twice with chloroform. The RNA concentration was determined using a NanoDrop cuvette-free spectrophotometer. cDNA was transcribed using Superscript II reverse transcriptase (Invitrogen, Carlsbad, CA, USA). Primers used are listed in Table 1. Realtime PCR reactions were performed in 384-well plates using Sybr-Green dye in a Bio-Rad CFX384 Real-Time System. Each sample was run in duplicate and the average was taken for calculation (Fig. 2.1). The housekeeping gene glyceraldehyde 3-phosphate dehydrogenase (*Gapdh*) was used as a loading control to normalize the expression of other genes. Two placental markers, *Mash2* (mammalian achaete scute-like homologue 2) [24] and *Tpbpa* (trophoblast specific protein alpha) [25], and a second



housekeeping gene *Hprt1* (hypoxanthine phosphoribosyltransferase 1) were also included as controls for placental development and loading control, respectively.

In situ hybridization. *In situ* hybridization was done following the standard laboratory procedure [26]. Frozen WT D13.5 placentas were sectioned at 10 μ m and mounted on Superfrost Plus slides. The sections were fixed in 4% paraformaldehyde and washed in 1xPBS. Sections were treated with 1% Triton X-100 and washed in 1xPBS. After pre-hybridization in a solution of 50% formamide and 5xSSC, sections were hybridized in a buffer of 5xSSC, 50% formamide, BSA, yeast tRNA, 10% dextran sulfate, and DIG-labeled antisense or sense RNA probe at 55°C. Sections were then washed in formamide/SSC solutions. After blocking for 1 hour with 1% blocking reagent, sections were incubated with anti-DIG antibody. Signal was visualized with 2 mM levamisole and 0.4 mM NBT/BCIP in a buffer of Tris-HCl, NaCl, and MgCl₂. Positive signal is dark brown (Fig. 2.2). Sections were counterstained with methyl green. Antisense and sense probes were synthesized using primers listed in Table 1.



Histology. Formalin fixed D13.5 placentas from WT females mated with *Lpar3*^{-/-} stud males and *Lpar3*^{-/-} females mated with WT stud males were sent to University of Georgia's Comparative Pathology Laboratory for processing and analysis by a

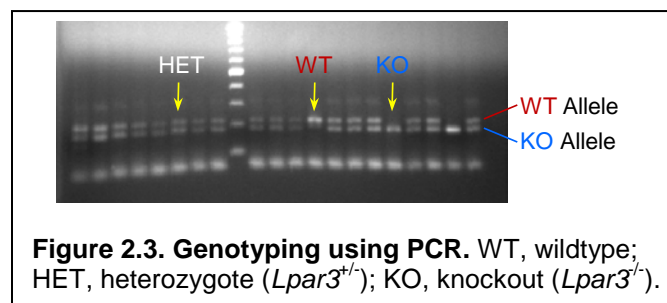
pathologist. Briefly, sagittal sections of paraffin-embedded placentas were cut at 5 μm and stained with hematoxylin and eosin.

Statistics. Realtime PCR data were analyzed using IBM SPSS Statistics 23. One way ANOVA followed by Dunnett's T3 test (*Lpar3*) or Tukey's test (*Mash2*, *Tpbpa*, *Hprt1*) were used. The significant level was set at $p < 0.05$.

2.4 Results

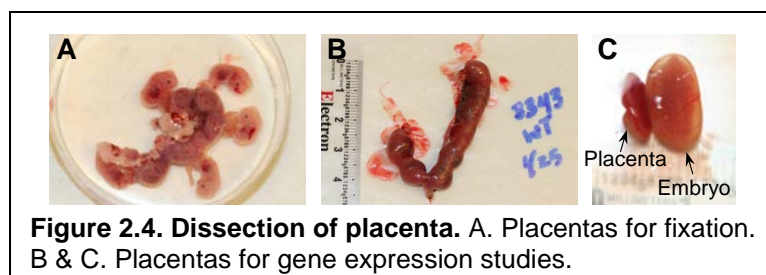
Genotyping

Mice were tailed and ear-tagged on postnatal day 21. Genotyping was done as previously described using PCR (Fig. 2.3) [10].



Dissection of placenta

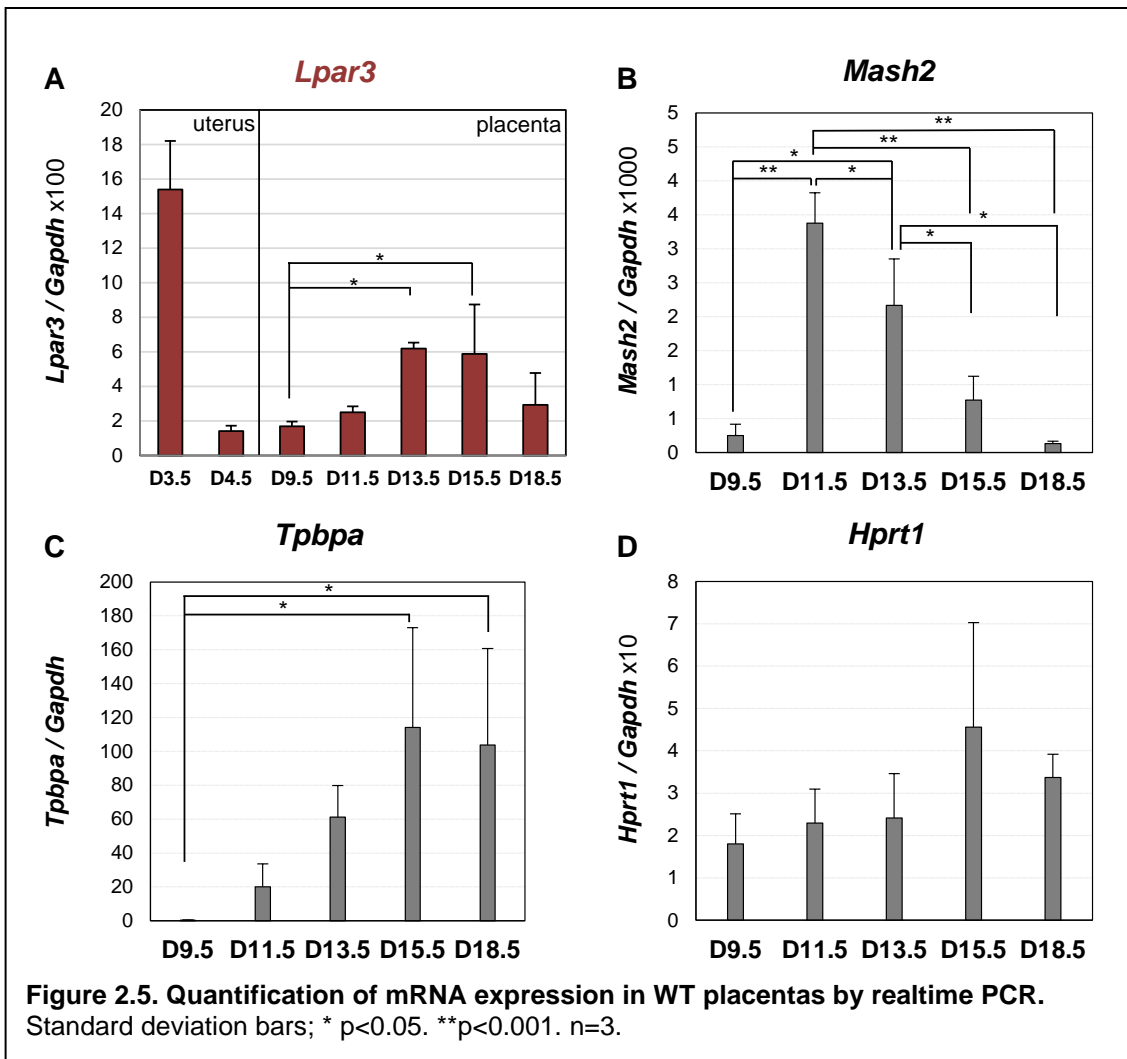
The pregnant control and *Lpar3*^{-/-} females were dissected at the designated time points, e.g., D9.5, D11.5, D13.5, D15.5, and D18.5. The uterus, placenta, and embryo remained as a single unit for formalin fixation (Fig. 2.4A), and later the placenta was dissected out for histology. Other placentas were isolated and frozen (Fig. 2.4B, 2.4C)



for realtime PCR and *in situ* hybridization. In control and *Lpar3*^{-/-} females, the placentas were on the mesometrial side as expected.

Temporal expression of Lpar3 mRNA in wild type placentas

Realtime PCR was conducted on D9.5, D11.5, D13.5, D15.5, and D18.5 WT placentas using the primers indicated in Table 1. *Lpar3* mRNA expression increased from D9.5 to D13.5 when the expression level plateaued (Fig. 2.5A). There was a slight but not significant decrease from D15.5 to D18.5. The downregulation of *Lpar3* mRNA from D3.5 uterus to D4.5 uterus was used as a control (Fig. 2.5A). *Mash2* gene, which encodes a basic helix-loop-helix transcription factor, is required for maintenance of giant

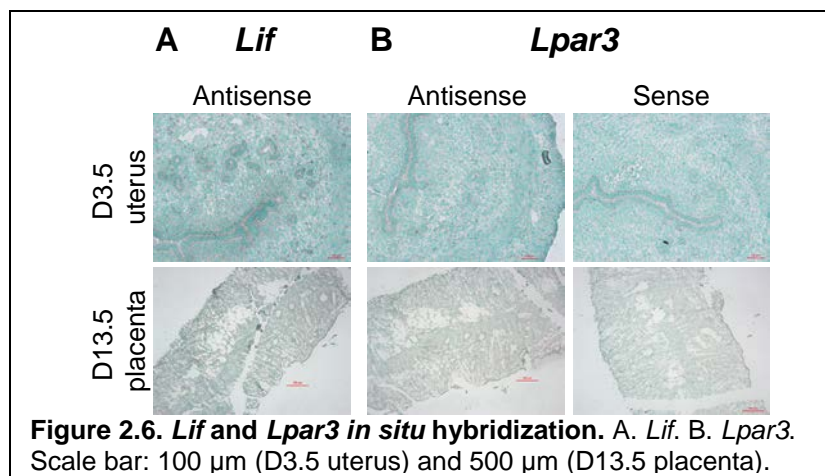


cell precursors and for development of the spongiotrophoblast to form a functional placenta [24]. *Mash2* expression sharply increased from D9.5 to D11.5 and gradually decreased afterwards (Fig. 2.5B). *Tpbpa* encodes a trophoblast-specific protein that is expressed in ectoplacental cone cells and later in the spongiotrophoblast layer of the mature placenta [25]. As expected, *Tpbpa* expression dramatically increased from D9.5 to D15.5 and then leveled off (Fig. 2.5C). The second housekeeping gene, *Hprt1*, did not show significant differential expression from D9.5 to D18.5 (Fig. 2.5D). These data demonstrate upregulation of *Lpar3* mRNA in the mouse placenta during placental development.

Localization of Lpar3 mRNA in wild type placentas

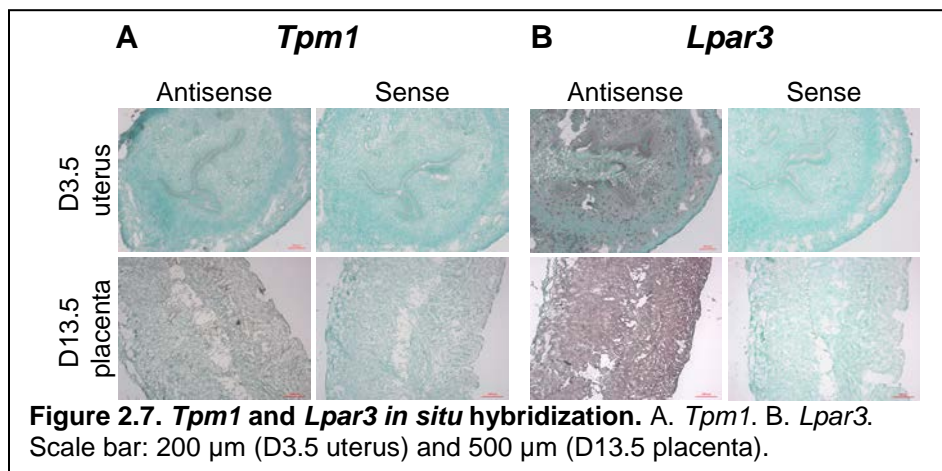
Since *Lpar3* mRNA expression peaked starting on D13.5 (Fig. 2.5A), D13.5 WT placenta was used for *in situ* hybridization to determine the localization of *Lpar3* mRNA. *Lpar3* mRNA was previously demonstrated to be specifically expressed in the D3.5 WT uterine luminal epithelium (LE) [10], so D3.5 WT uterus was used as the positive control tissue.

Three probes were used in the first *in situ* hybridization experiment: *Lif* antisense probe, *Lpar3* antisense probe, and *Lpar3* sense probe. *Lif* (leukemia inhibitory factor)



mRNA is highly expressed in the glandular epithelium (GE) [27], so the *Lif* antisense probe was included as a positive control. *Lif* antisense probe did detect weak signal in GE of D3.5 uterus, but there was also signal in LE (Fig. 2.6A). There was some weak signal in LE of D3.5 uterus using *Lpar3* antisense probe, but the signal was not distinguishable between *Lpar3* antisense probe and *Lpar3* sense probe in both D3.5 uterus and D13.5 placenta (Fig. 2.6B). Presence of signal after using the sense probe indicated that this set of experiments was not successful.

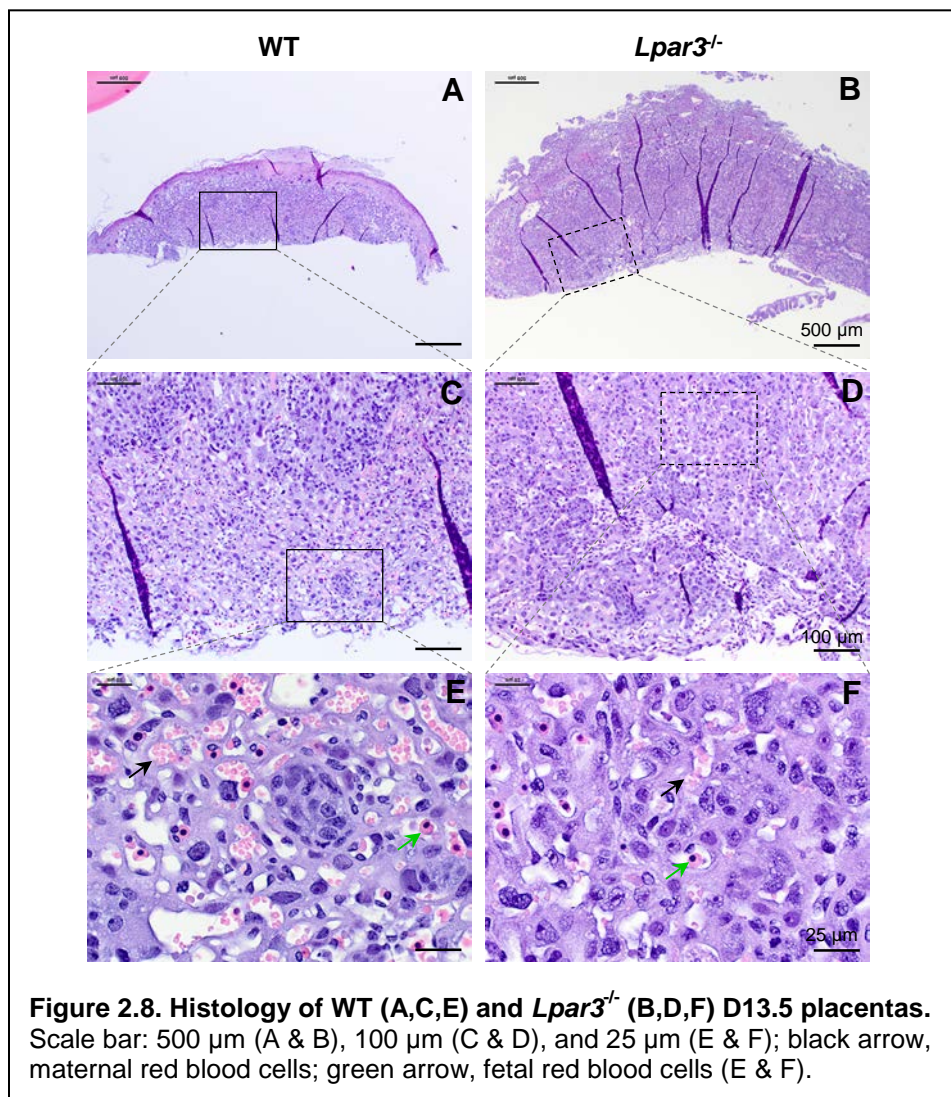
In the second experiment, *Tpm1* (Tropomyosin 1) was used as a positive control. *Tpm1* is highly expressed in LE, GE, and myometrium [28]. In this set of experiments, there were signals using *Tpm1* antisense probe and *Lpar3* antisense probe but no specific signal using *Tpm1* sense probe and *Lpar3* sense probe (Fig. 2.7). However, the issue was that the weak signal detected by *Tpm1* antisense was mainly in LE and the strong signal detected by *Lpar3* antisense probe was not confined in LE of D3.5 WT uterus. Also, the *Lpar3* antisense probe detected signal throughout the D13.5 placenta (Fig. 2.7B). Because the positive controls did not work, no conclusion could be made about *Lpar3* mRNA localization in D13.5 WT placenta.



D13.5 *Lpar3*^{-/-} placenta histology

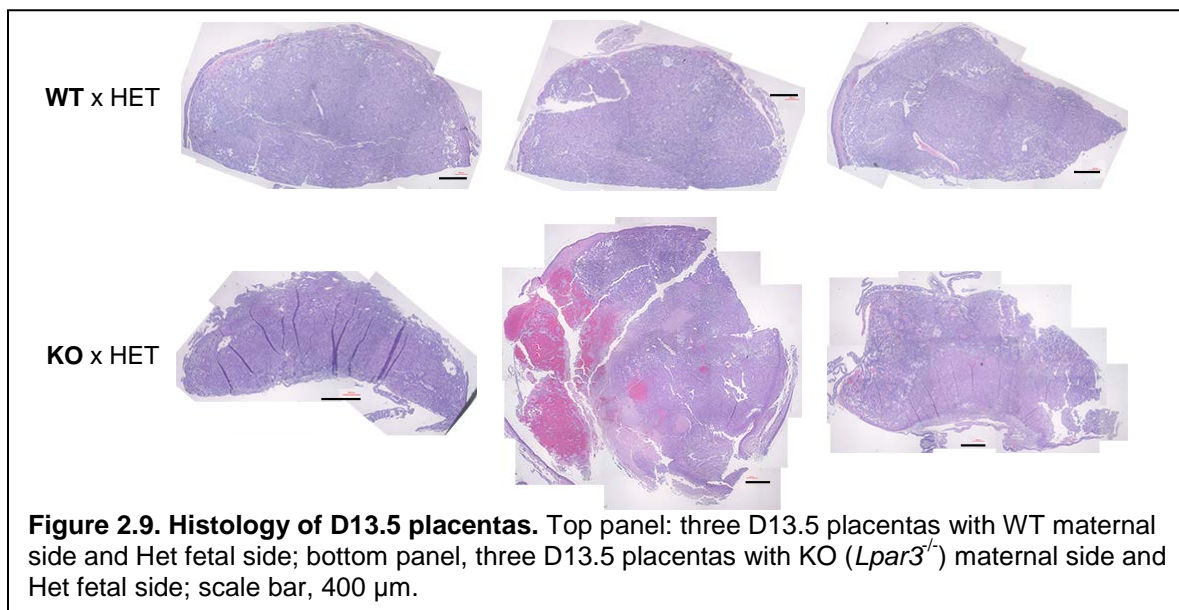
Since the placental hypertrophy was only observed in the *Lpar3*^{-/-} females and was unrelated to the genotypes of the embryos [10], we hypothesized that this phenotype was caused by the loss of LPA₃ in the maternal side.

In the first histology study, the placentas were from WT and *Lpar3*^{-/-} females, but the genotypes of the fetal side were not determined. Histology of these D13.5 placentas demonstrated that singleton or conjoined placentas from *Lpar3*^{-/-} maternal sides had similar abnormalities, including a very dense spongiotrophoblast layer and reduced



numbers of vascular channels in the spongiotrophoblast layer compared to WT control (Fig. 2.8 and data not shown). It appeared that there was more reduction of vascular channels for maternal blood than for fetal blood in the spongiotrophoblast layer of D13.5 *Lpar3*^{-/-} placenta (Fig. 2.8F) compared to WT placenta (Fig. 2.8E).

In the second histology study, D13.5 placentas were collected from WT females mated with *Lpar3*^{-/-} stud males and *Lpar3*^{-/-} females mated with WT stud males. These placentas had WT or *Lpar3*^{-/-} maternal tissue, respectively, and all had HET (*Lpar3*^{+/-}) fetal tissue. Because these placentas were sectioned at inconsistent angles (Fig. 2.9), systematic analysis of the different layers could not be done.



2.5 Discussion

The preliminary histology data from the first set of placentas suggest compromised placental development in the *Lpar3*^{-/-} females. Because of the heterogeneity of the placenta, it is important to control the genotypes of the maternal side and fetal side and to have comparable sections from different placentas for

systematic comparisons. The second set of placentas had the same fetal genotype of Het with the only genotypic difference on the maternal side. This was based on the observation that placental hypertrophy was associated with the maternal genotype [10]. The sections from the second set of placentas were unfortunately sectioned at varying angles so no meaningful conclusions could be made. These experiments will be repeated with appropriately sectioned tissues.

The increase of *Lpar3* expression from D9.5 to D13.5 prompted us to analyze the localization of *Lpar3* in the D13.5 placenta. Because our lab has not been able to identify an LPA₃ antibody that works in immunohistochemistry, we turned to *in situ* hybridization that detects mRNA localization. Unfortunately we have not been successful with this difficult technique. The main reason might be the quality of the probes. A lab mate Ahmed did *in situ* hybridization on D13.5 WT placenta using *Lpar3* antisense and sense probes. He detected signals using *Lpar3* antisense probe but not *Lpar3* sense probe in the placenta (data not shown). The signals were mainly localized in the junctional zone and labyrinth zone with only sporadic signals in the decidua. If this pattern of expression is confirmed to be correct, it would indicate that the spatiotemporal expression of *Lpar3* corresponds to the vasculature development of the placenta. Reduced numbers of vascular channels, especially those for maternal blood in the spongiotrophoblast layer, supports a potential role of maternal LPA₃ in the placental vasculature development. However, the mechanism is unknown.

One potential mechanism involves the role of LPA₃ ligand LPA in promoting angiogenesis [29], a process of branching and elongating previously existing vessels to make new blood vessel networks that is important for placental development [30]. Since

there is reduced vascular space in the spongiotrophoblast layer of the junctional zone, we speculated that maternal LPA₃ may have a direct effect on angiogenesis during placental development. However, the cell types that express *Lpar3* in the junctional zone remain unidentified. Another possible mechanism may involve the invading trophoblasts, which are essential for placental vasculature development [30]. Maternal LPA₃ may have an indirect effect on placental development by promoting invading trophoblasts through an unknown paracrine mechanism. The development of the maternal and fetal circulation in the placentas from *Lpar3*^{-/-} females remains to be determined. Defective maternal circulation would suggest a direct effect of LPA₃, and defective fetal circulation would suggest an indirect effect. Regardless, placental hypertrophy seen in *Lpar3*^{-/-} females could be a compensatory effect of placental insufficiency caused by abnormal placental vasculature development. At this stage, the data suggest a connection between LPA₃ signaling and placental development, but further studies must be done to prove a possible link.

Table 1. Primers used in the study.

Gene	Primer	Experiment
<i>A3e1b</i>	TGACAAGCGCATGGACTTTTTTC	Genotyping
<i>A3e1c</i>	GAAGAAATCCGCAGCAGCTAA	
<i>Neo1b</i>	AGCGCCTCCCCTACCCGGTAGAAT	
<i>Lpar3</i> (LPA3e2F2)	ACACCAGTGGCTCCATCAG	Realtime PCR <i>In situ</i> hybridization
<i>Lpar3</i> reverse (LPA3e3R2)	GTTTCATGACGGAGTTGAGCAG	
<i>Mash2</i> (mMash2eF1)	GCGTAAAGCTGGTAAACTTG	Realtime PCR
<i>Mash2</i> reverse (mMash2eR1)	CCCTAACCAACTGGAAAAGT	
<i>Tpbpa</i> (mTpbpae2F1)	CCTACAATCTTCCTAGTCATCC	
<i>Tpbpa</i> reverse (mTpbpae4R1)	TCGCCACTCTCTGTGTAATC	
<i>Hprt1</i> (HPRT1e3F1)	GCTGACCTGCTGGATTACAT	
<i>Hprt1</i> reverse (HPRT1e4/5R1)	CAATCAAGACATTCTTTCCAGT	
<i>Gapdh</i> (mGapdhe3F1)	GCCGAGAATGGGAAGCTTGTCAT	
<i>Gapdh</i> reverse (mGapdhe4R1)	GTGGTTCACACCCATCACAAACAT	
<i>Lif</i> (mLife2F4)	GCCATAATGAAGGTCTTGG	<i>In situ</i> hybridization
<i>Lif</i> reverse (mLife4R4)	CCAAGTTGGTCTTCTCTGTC	
<i>Tpm1</i> (mTpm1e2F1)	GGTGTCAGTGC AAAAGAAAC	
<i>Tpm1</i> reverse (mTpm1e5R1)	CTCGATGATGACCAGCTTAC	

CHAPTER 3

ERK EXPRESSION in *Lpar3*^{-/-} MOUSE UTERUS during EMBRYO IMPLANTATION²

² Dudley, EA; Li, R; El Zowalaty, AE; Wang, Z; and Ye, X. To be submitted to Biology of Reproduction

3.1 Abstract

Lysophosphatidic acid (LPA) is a signaling molecule that acts through six GPCRs, LPA₁₋₆. They couple to different G proteins to activate downstream signaling cascades. LPA₃ couples to G_q and G_i. One of the G_i downstream signaling molecules is ERK (extracellular signal-regulated kinase or mitogen-activated protein kinase (MAPK)). A main function of ERK signaling is to promote cell proliferation. ERK signaling has been implicated in uterine preparation for embryo implantation. Implantation initiates on D4.0 in mice. Mice without LPA₃ (*Lpar3*^{-/-}) have defective embryo implantation due to a uterine defect. There is decreased stromal cell proliferation in the gestation day 3.5 (D3.5) *Lpar3*^{-/-} uterus. Therefore, we hypothesize that LPA₃-mediated signaling may promote uterine stromal cell proliferation to prepare the uterus for embryo implantation via ERK phosphorylation. Uterine tissues from pregnant D3.5 control (*Lpar3*^{+/+} (WT) and *Lpar3*^{+/-} (HET)) and *Lpar3*^{-/-} mice were collected. Western blotting showed two bands of total-ERK1/2 (tERK) and two bands of phospho-ERK1/2 (pERK). There were individual variations in the intensity of the bands but no obvious difference between the two groups. Immunohistochemistry indicated that tERK signal was mainly detected in the uterine epithelium with weaker expression in uterine stroma and myometrium of control and *Lpar3*^{-/-} mice. There was no obvious difference between the two groups. Immunohistochemistry for pERK failed to detect any specific signal. The same patterns were also observed in positive tissue control D5.5 WT uterus. No signal was detected in the negative control. These preliminary data indicate that the overall ERK signaling is not altered in the preimplantation D3.5 *Lpar3*^{-/-} uterus. Because the pERK antibody failed to detect specific signal in the uterine sections, any spatiotemporal change of

pERK in the *Lpar3*^{-/-} uterus is still undetermined. The role of LPA₃ signaling through ERK phosphorylation to prepare the uterus for embryo implantation remains unknown.

3.2 Introduction and Literature Review

Lysophosphatidic acid (LPA) is a simple phospholipid that can be found in many biological fluids including serum, plasma, and tears and can be produced in various cell types [3, 4]. LPA can activate six GPCRs, LPA₁-LPA₆ [3, 6]. *Lpar3*, the gene for LPA₃ in mice, has been detected in the oviduct, placenta, and uterus of the female reproductive system [10]. LPA₃ is involved in uterine smooth muscle contraction which may influence both embryo spacing at the beginning of pregnancy and parturition at the end of the pregnancy [5].

Lpar3 and LPA₃ have been detected in the embryo and uterus during the periimplantation period in multiple animal models. In sheep, LPA₃ has been detected in the luminal and glandular epithelium in the uterus and in the trophectoderm of the embryo, suggesting a role for LPA signaling in embryo elongation and implantation [3]. Similarly in pigs, *Lpar3* expression peaks when the embryo elongates prior to implantation and is found in the luminal and glandular epithelium [5]. In mice, *Lpar3* mRNA expression peaked on gestation day 3.5 (D3.5) and was mainly found in the luminal epithelium (LE) of the uterus [10].

LPA₃ plays a critical role in mouse embryo implantation. Deletion of *Lpar3* in mice (*Lpar3*^{-/-}) leads to delayed uterine receptivity for embryo implantation, embryo crowding, increased post-implantation embryonic death, and reduced litter size. These phenotypes are unrelated to the genotypes of the mating males, indicating maternal

defects [10]. *Lpar3* is the only LPA receptor that has greatly increased expression during the periimplantation period, and it is localized to the LE which is the first layer of cells the blastocyst communicates with during implantation. Thus, LPA₃ is likely involved in the establishment of uterine receptivity to the implanting embryos [13].

LPA₃ couples to G_q and G_i, and one of the G_i downstream signaling molecules is ERK (extracellular signal-regulated kinase or mitogen-activated protein kinase (MAPK)). A main function of ERK signaling is to promote cell proliferation. ERK signaling has been implicated in uterine preparation for embryo implantation [31]. We found decreased stromal cell proliferation in the gestation day 3.5 (D3.5) *Lpar3*^{-/-} uterus [16]. Therefore, we hypothesize that LPA₃-mediated signaling may promote uterine stromal cell proliferation to prepare the uterus for embryo implantation via ERK phosphorylation. This hypothesis was tested in D3.5 *Lpar3*^{-/-} mouse uterus.

3.3 Materials and Methods

Animals. Wild type (WT), *Lpar3* heterozygous (*Lpar3*^{+/-} / Het), and *Lpar3*^{-/-} (hom) mice in a mixed background (129/SvJ and C57BL/6) were generated from a colony at the University of Georgia which was originally derived at The Scripps Research Institute. The mice were housed in polypropylene cages with free access to food and water from water sip tubes with a reverse-osmosis system. The animal facility has 12 hour light:dark days with 30%-50% relative humidity at 23±1°C. All methods used in this study were approved by the University of Georgia Institutional Animal Care and Use Committee and conform to National Institutes of Health guidelines and public law.

Females were naturally mated with WT stud males. The day a plug was found was designated D0.5.

Tissue collection. Mated adult females were dissected on D3.5 when *Lpar3* mRNA expression peaked in WT uterus [10] and reduced stromal proliferation was detected [16] prior to embryo attachment, which occurred on D4.0. D5.5 WT uterus was collected as a positive control tissue. Uterine tissues were flash frozen and stored at -80°C. Tissues were genotyped as shown in Section 2.4 Results.

Western blot. Uterine tissue was homogenized in RIPA buffer with 1% protease inhibitor. Protein concentrations were determined using Quick Start Bradford Protein Assay with a Nanodrop spectrophotometer. Samples were mixed with Laemmli buffer and heated at 95°C for 5 minutes. Samples were run on any kDa Mini-Protein TGX gels (Bio-Rad) and transferred to polyvinylidene fluoride (PVDF) membranes using a Trans-Blot SD Semi-Dry Electrophoretic Transfer Cell (Bio-Rad). Membranes were then blocked in 5% non-fat milk in Tris-buffered saline with 0.5% Tween-20 (TBST) for 1 hour. Blocked membranes were incubated overnight at 4°C with total-ERK1/2 (p44/42 MAPK, Cell Signaling #4695) or phospho-ERK1/2 (phospho-p44/42 MAPK, Cell Signaling #4370) antibodies in 5%BSA in TBST. After washing with TBST, membranes were incubated with the appropriate secondary antibody for 1 hour at room temperature. To visualize the bands, membranes were incubated with Pierce ECL Western Blotting Substrate (Thermo Scientific #32106) for one minute and placed with film in a cassette for an optimized amount of time. The film was developed and scanned into a computer.

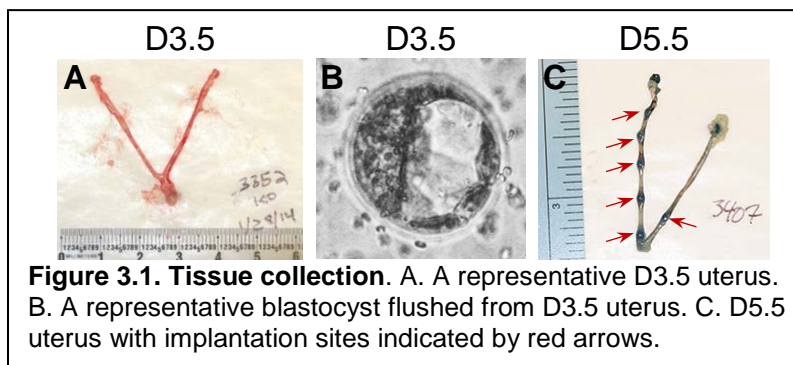
Immunohistochemistry. Immunohistochemistry was done as previously described [16, 32-34]. Frozen D3.5 WT and *Lpar3*^{-/-} uteri were cross-sectioned. The

uterine sections (10 μm) were immunostained for total-ERK1/2 (p44/42 MAPK, Cell Signaling #4695) or phospho-ERK1/2 (phospho-p44/42 MAPK, Cell Signaling #4370) with a negative control containing no primary antibody. WT D5.5 uterine sections were used as a positive control.

3.4 Results

Uterus collection and pregnancy status

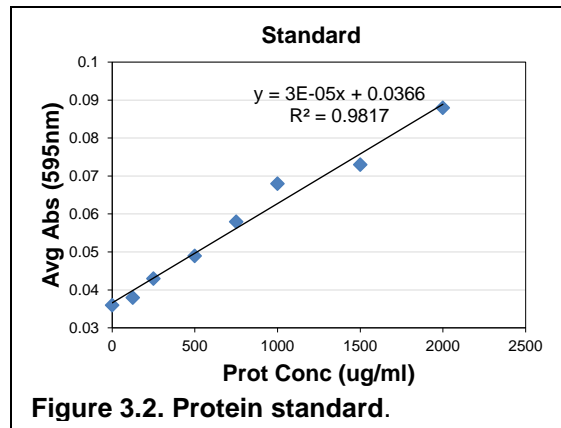
D3.5 WT and *Lpar3*^{-/-} (Fig. 3.1A) uteri were collected. Since not all mated females were pregnant and only pregnant females were used in the study, the uterine horns were flushed and checked for the presence of blastocysts (Fig. 3.1B) to determine pregnancy status. A D5.5 uterus was collected as a positive tissue control for immunohistochemistry (Fig. 3.1C).



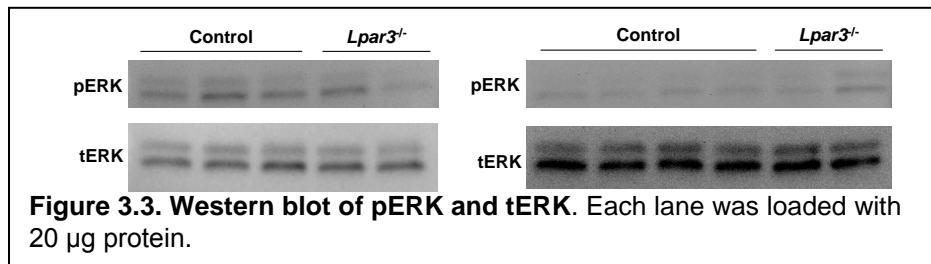
Western blot

Protein was extracted from each uterus. Protein concentrations were determined according to a standard shown in Fig. 3.2.

After the conditions for phospho-ERK (pERK) and total-ERK (tERK) were optimized for western blot (data not shown), seven D3.5 control and four D3.5 *Lpar3*^{-/-} uterine samples were run in two gels for detecting pERK and tERK (Fig. 3.3). The



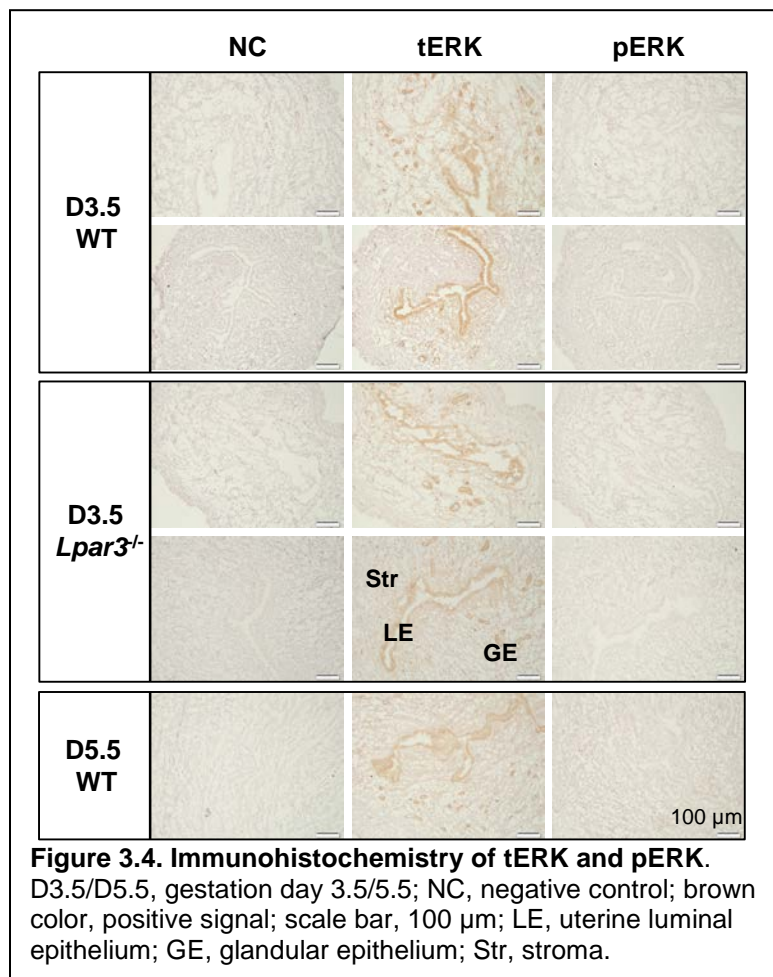
western blot analysis showed two bands between two size markers of 36 kDa and 47 kDa but closer to 47 kDa, consistent with the expected sizes of 42 kDa and 44 kDa. There were variations of the intensity of the bands among different samples, but there was no obvious difference in pERK or tERK between control and *Lpar3*^{-/-} uteri. Total-ERK served as a loading control. Amido Black total protein stain was used as a secondary loading control (data not shown).



Immunohistochemistry

Although western blotting did not reveal consistent difference in pERK expression between D3.5 control and *Lpar3*^{-/-} pregnant uteri (Fig. 3.3), it was possible that there was changed pERK expression in the different uterine compartments of *Lpar3*^{-/-} uterus. Immunohistochemistry was done on two D3.5 WT pregnant uteri, two D3.5 *Lpar3*^{-/-} pregnant uteri, and one D5.5 WT pregnant uterus. Two sections from each uterus were included. No specific signal was detected in the negative control. Total-ERK was mainly detected in the uterine epithelium, including luminal epithelium and

glandular epithelium; weaker expression was detected in the stroma and myometrium. There was no obvious difference between WT and *Lpar3*^{-/-} uteri (Fig. 3.4). Unfortunately, our pERK antibody did not detect any specific signal in all uterine sections. These experiments were repeated with the same results (data not shown).



3.5 Discussion

Seven control and four *Lpar3*^{-/-} D3.5 uterine samples were included in the western blot study. Although there were individual variations, we observed no consistent change between the two groups. Perhaps a larger sample size will show a significant difference. Total-ERK (tERK) and phospho-ERK (pERK) showed bands with the

expected sizes in the western blots, indicating that the antibodies were specific. However, compared to tERK signal, it took a longer time for the pERK signal to develop on the film, indicating that either the pERK antibody is weaker than the tERK antibody or that there is less pERK present in the sample.

Immunohistochemistry detected no specific pERK signal in any of the uterine sections, but tERK signal was strong in the uterine epithelium. There are three potential reasons for our findings. Firstly, the pERK antibody may be too weak to detect any signal in the uterine tissue using this method. Secondly, the pERK signal may be unstable and was lost during uterine section preparation causing low pERK signal detection. Thirdly, despite strong tERK signal in uterine sections, there may be limited ERK phosphorylation in the tissue leading to low pERK signal. However, the third potential reason is less likely because another study has demonstrated that pERK signal is detectable in the mouse uterus during embryo implantation [31].

A uterus contains different cellular compartments, such as epithelium, stroma, and myometrium. When a protein has spatiotemporal cellular specific expression in the uterus during embryo implantation, such as progesterone receptor [16, 32] and estrogen receptor alpha [16], the spatiotemporal cellular expression will give more insightful information than the overall uterine expression levels. Since the immunohistochemistry of pERK did not work, no conclusion could be made about whether or not deletion of *Lpar3* will affect ERK signaling and whether or not ERK signaling is important in mediating LPA₃ signaling in uterine stromal cell proliferation [16] in preparation for embryo implantation. A better pERK antibody would need to be used to form a conclusion in the future. Alternatively, a different signaling molecule in the LPA₃-ERK

pathway or molecules in the LPA₃-Gi downstream signaling pathways (Fig. 1.2) [6] can be investigated to determine a potential molecular mechanism of LPA₃ in uterine stromal cell proliferation [16].

CHAPTER 4

COLLABORATIVE WORK

The main focus of Dr. Ye's lab is embryo implantation with a secondary focus on the effects of endocrine disruptors on different aspects of pregnancy. Each PhD student in the lab developed projects branching from these two main topics. During my MS study, I have been involved in several projects that were led by my lab mates. Below is a list of the projects in which I was involved.

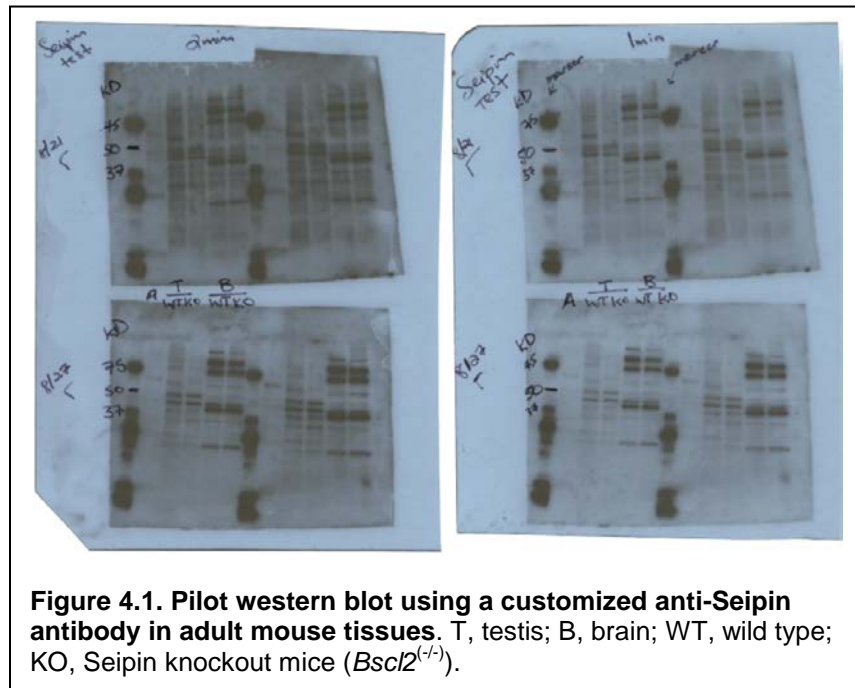
1. Zhao, F., Zhou, J., El Zowalaty, A.E., Li, R., **Dudley, E.A.**, Ye, X., 2014. Timing and recovery of postweaning exposure to diethylstilbestrol on early pregnancy in CD-1 mice. *Reprod Toxicol* 49, 48-54.

My contribution: Over 100 female mice were used in the study. Dissection was a team effort. My main contribution in this project was dissection.

2. Li, R., El Zowalaty, A.E., Chen, W., **Dudley, E.A.**, Ye, X., 2015. Segregated responses of mammary gland development and vaginal opening to prepubertal genistein exposure in *Bsc12*^(-/-) female mice with lipodystrophy. *Reprod Toxicol* 54, 76-83.

My contribution: I did pilot western blotting to test an anti-Seipin antibody (Seipin is encoded by the *Bsc12* gene). I extracted proteins from adult testis and brain of WT and Seipin knockout male mice (*Bsc12*^(-/-)). Most likely because of the nature of this protein or the antibody, neither our collaborator Dr. Chen (who provided this customized antibody) at Georgia Regents University (now Augusta University) nor I could get a suitable

condition for western blotting (Fig. 4.1). However, this antibody could detect specific signals in WT testis but not in Seipin knockout testis using immunohistochemistry (done by my lab mate Ahmed El Zowalaty). Immunohistochemistry results were included in the paper.

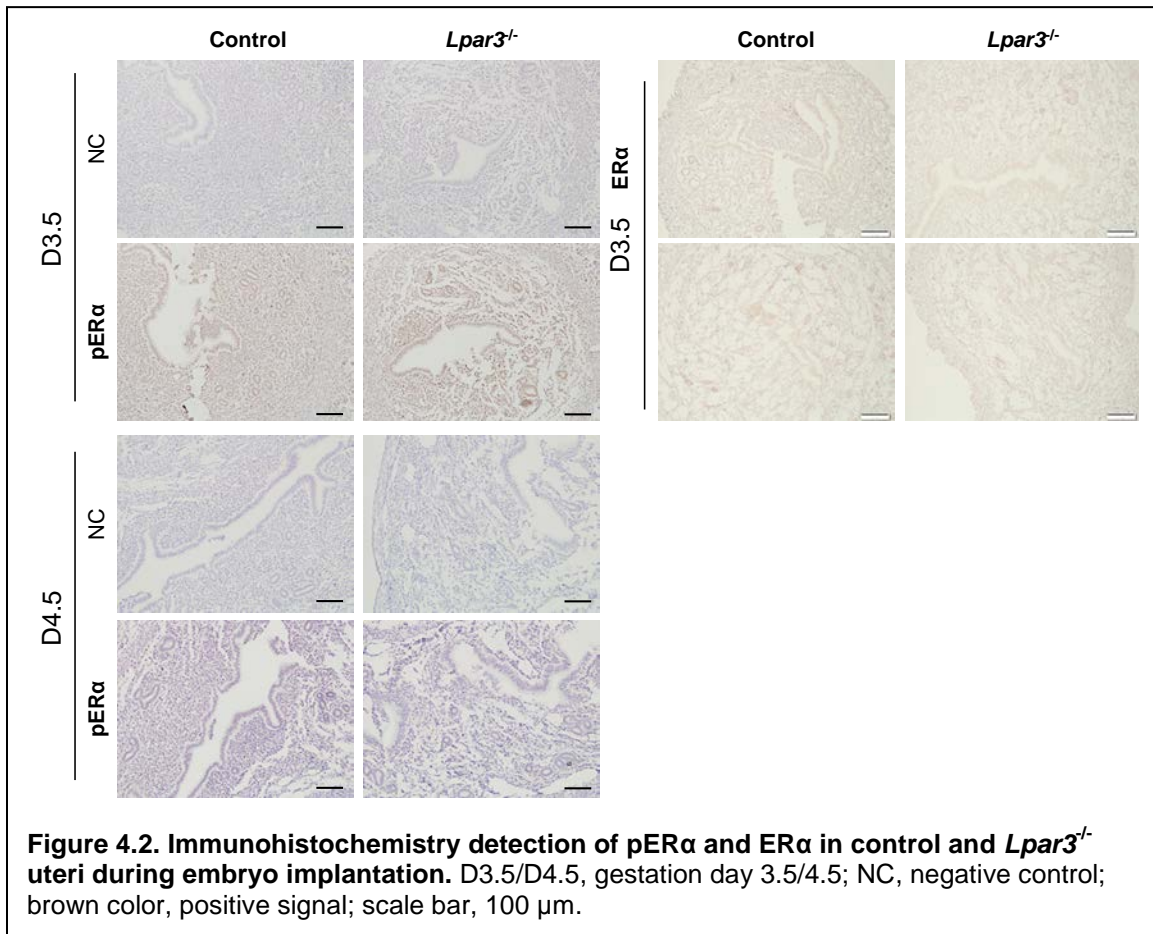


- Li, R., Diao, H., Zhao, F., Xiao, S., El Zowalaty, A.E., **Dudley, E.A.**, Mattson, M.P., Ye, X., 2015. Olfactomedin 1 Deficiency Leads to Defective Olfaction and Impaired Female Fertility. *Endocrinology* 156, 3344-3357.

My contribution: I was involved in animal care and troubleshooting with immunohistochemistry (data not shown in the paper).

- Diao, H., Li, R., El Zowalaty, A.E., Xiao, S., Zhao, F., **Dudley, E.A.**, Ye, X., 2015. Deletion of Lysophosphatidic Acid Receptor 3 (Lpar3) Disrupts Fine Local Balance of Progesterone and Estrogen Signaling in Mouse Uterus During Implantation. *Biol Reprod.*

My contribution: I tested different antibodies using immunohistochemistry and added more replicates on the expression of estrogen receptor alpha (ER α) and phosphorylated ER α (pER α) in WT and *Lpar3*^{-/-} uteri during embryo implantation (Fig. 4.2). In the publication above, pER α data were not included, and ER α immunohistochemistry data were from the set done by former lab mate Honglu Diao.

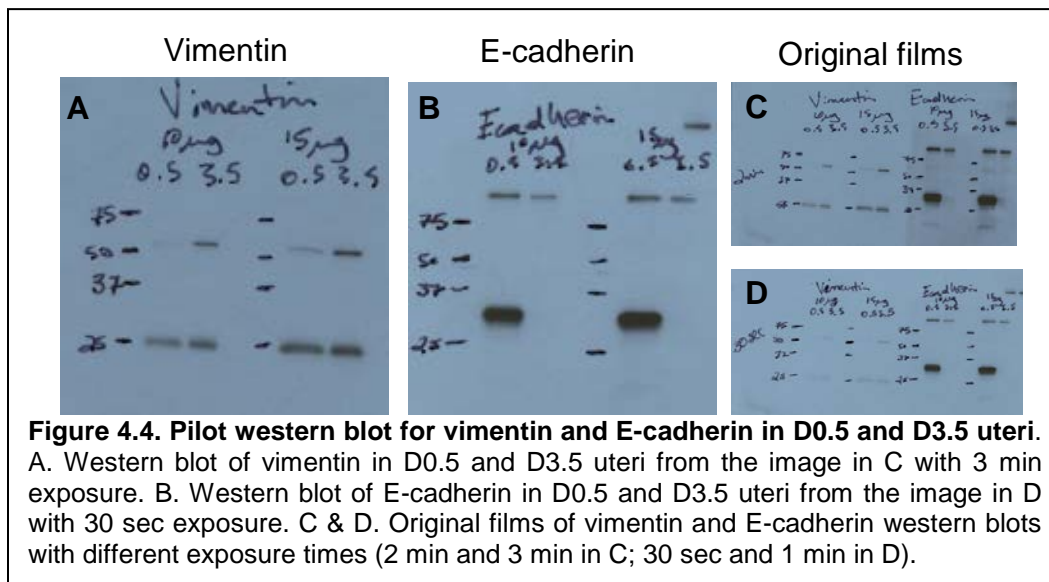


5. Zhao, F., Zhou, J., Li, R., **Dudley, E.A.**, Ye, X., LHFPL2 is essential for distal reproductive tract development in mice. Submitted to “*Scientific Reports*”

My contribution: I did half of the fertility test in control and LHFPL2 mutant male mice. A. I checked vaginal plugs every morning and recorded the plugging latency (Fig. 4.3A) to determine the mating activities of the male mice. B. I monitored the pregnancy of the

6. Li, R., **Dudley, E.A.**, Ye, X., Epithelial-mesenchymal transition (EMT) in mouse uterus during early pregnancy. Ongoing project.

My contribution: This is a pilot study in collaboration with my lab mate Rong Li to investigate whether EMT/MET occurs in the uterus during early pregnancy. I isolated protein from gestation day 0.5 (D0.5) and D3.5 mouse uteri and loaded 10 μ g and 15 μ g to optimize the western blotting protocol. Vimentin, around 55 kDa, is a marker for mesenchymal cells. The band was darker in the D3.5 lanes than in the D0.5 lanes (Fig. 4.4A). Interestingly, this antibody also detected an unknown band at 25 kDa (Fig. 4.4A). E-cadherin, 135 kDa, is a marker for epithelial cells. The levels were visibly lower in the D3.5 lanes (Fig 4.4B). Surprisingly, there was a very strong band at 30 kDa detected in the D0.5 uterus but not in the D3.5 uterus (Fig 4.4B). We have not been able to identify this band or why it is only present in the D0.5 uterus.



CHAPTER 5

Conclusion

During my Master's study, I led two projects in determining the role of LPA₃ in placental development using our *Lpar3*^{-/-} mouse model (Chapter 2) and ERK signaling in the *Lpar3*^{-/-} uterus during embryo implantation (Chapter 3); I also worked on several collaborative projects (Chapter 4) yielding four co-authored papers and two more manuscripts under review/in preparation.

Preliminary data on the role of LPA₃ in placental development (Chapter 2) show upregulation of *Lpar3* mRNA during placenta development and a very dense spongiotrophoblast layer with reduced numbers of vascular channels in the *Lpar3*^{-/-} females, suggesting a potential role of LPA₃ in placenta development. The localization of *Lpar3* in the developing placentas and the molecular mechanism of LPA₃-mediated signaling in placental development are still not clear. In addition to repeating the experiments in Chapter 2, future studies for this project may include realtime PCR analysis of genes involved in placental development in the *Lpar3*^{-/-} tissue, immunohistochemistry of control and *Lpar3*^{-/-} tissues to determine any differences in proteins involved in placental development, and *in situ* hybridization with cell-specific genes to determine which cell types may be involved in the altered placenta development in the *Lpar3*^{-/-} mice.

Preliminary data on ERK signaling (Chapter 3) suggest that overall ERK signaling is not altered in the preimplantation D3.5 *Lpar3*^{-/-} uterus. Because our pERK

antibody failed to detect any specific signal in the uterine sections, it remains undetermined whether there is any spatiotemporal change of ERK phosphorylation in the *Lpar3*^{-/-} uterus and whether ERK signaling might be important for LPA₃ in preparing the uterus for embryo implantation. Besides the ERK immunohistochemistry, future study in this project may include immunohistochemistry of other proteins in the LPA₃ pathway.

REFERENCES

1. Watson, E.D. and J.C. Cross, *Development of Structures and Transport Functions in the Mouse Placenta*. Physiology, 2005: p. 180-193.
2. Simmons, D.G., *Postimplantation Development of the Chorioallantoic Placenta*, in *The Guide to the Investigation of Mouse Pregnancy*, B. Croy, et al., Editors. 2014, Elsevier. p. 143-162.
3. Woclawek-Potocka, I., et al., *Lysophosphatidic acid (LPA) signaling in human and ruminant reproductive tract*. Mediators Inflamm, 2014. **2014**: p. 649702.
4. Aoki, J., *Mechanisms of lysophosphatidic acid production*. Semin Cell Dev Biol, 2004. **15**(5): p. 477-89.
5. Ye, X. and J. Chun, *Lysophosphatidic acid (LPA) signaling in vertebrate reproduction*. Trends in Endocrinology and Metabolism, 2009: p. 17-24.
6. Choi, J.W., et al., *LPA receptors: subtypes and biological actions*. Annu Rev Pharmacol Toxicol, 2010. **50**: p. 157-86.
7. Chun, J., et al., *International Union of Basic and Clinical Pharmacology. LXXVIII. Lysophospholipid receptor nomenclature*. Pharmacol Rev, 2010. **62**(4): p. 579-87.
8. Aoki, J., A. Inoue, and S. Okudaira, *Two pathways for lysophosphatidic acid production*. Biochimica et Biophysica Acta, 2008: p. 513-518.
9. Iwasawa, Y., et al., *Expression of Autotaxin, an Ectoenzyme that Produces Lysophosphatidic Acid, in Human Placenta*. American Journal of Reproductive Immunology, 2009: p. 90-95.
10. Ye, X., et al., *LPA3-mediated lysophosphatidic acid signalling in embryo implantation and spacing*. Nature, 2005: p. 104-108.

11. Ye, X., et al., *Age-dependent loss of sperm production in mice via impaired lysophosphatidic acid signaling*. Biol Reprod, 2008. **79**(2): p. 328-36.
12. Ye, X., et al., *Unique uterine localization and regulation may differentiate LPA3 from other lysophospholipid receptors for its role in embryo implantation*. Fertil Steril, 2011. **95**(6): p. 2107-2113 e4.
13. Ye, X., et al., *Unique uterine localization and regulation may differentiate LPA3 from other lysophospholipid receptors for its role in embryo implantation*. Fertility and Sterility, 2011: p. 2107-2113.
14. Hama, K., et al., *Embryo Spacing and Implantation Timing Are Differentially Regulated by LPA3-Mediated Lysophosphatidic Acid Signaling in Mice*. Biol Reprod, 2007. **77**(6): p. 954-9.
15. Ye, X., H. Diao, and J. Chun, *11-deoxy prostaglandin F(2alpha), a thromboxane A2 receptor agonist, partially alleviates embryo crowding in Lpar3((-/-)) females*. Fertil Steril, 2012. **97**(3): p. 757-63.
16. Diao, H., et al., *Deletion of Lysophosphatidic Acid Receptor 3 (Lpar3) Disrupts Fine Local Balance of Progesterone and Estrogen Signaling in Mouse Uterus During Implantation*. Biol Reprod, 2015.
17. Tokumura, A., et al., *Increased production of bioactive lysophosphatidic acid by serum lysophospholipase D in human pregnancy*. Biol Reprod, 2002. **67**(5): p. 1386-92.
18. Masuda, A., et al., *Serum autotaxin measurements in pregnant women: application for the differentiation of normal pregnancy and pregnancy-induced hypertension*. Clin Chim Acta, 2011. **412**(21-22): p. 1944-50.
19. Iwasawa, Y., et al., *Expression of autotaxin, an ectoenzyme that produces lysophosphatidic acid, in human placenta*. Am J Reprod Immunol, 2009. **62**(2): p. 90-5.
20. Ichikawa, M., et al., *Placental autotaxin expression is diminished in women with pre-eclampsia*. J Obstet Gynaecol Res, 2015. **41**(9): p. 1406-11.

21. Li, L.X., et al., [*Expression and significance of Edg4 and Edg7 in the placentas of patients with hypertensive disorder complicating pregnancy*]. Zhonghua Fu Chan Ke Za Zhi, 2007. **42**(6): p. 386-9.
22. Cross, J., et al., *Trophoblast functions, angiogenesis and remodeling of the maternal vasculature in the placenta*. Molecular and Cellular Endocrinology, 2002: p. 207-212.
23. Woclawek-Potocka, I., et al., *Lysophosphatidic Acid (LPA) Signaling in Human and Ruminant Reproductive Tract*. Mediators of Inflammation, 2014.
24. Stepan, H., et al., *Structure and regulation of the murine Mash2 gene*. Biol Reprod, 2003. **68**(1): p. 40-4.
25. Hu, D. and J.C. Cross, *Ablation of Tpbpa-positive trophoblast precursors leads to defects in maternal spiral artery remodeling in the mouse placenta*. Dev Biol, 2011. **358**(1): p. 231-9.
26. Diao, H., et al., *Broad gap junction blocker carbenoxolone disrupts uterine preparation for embryo implantation in mice*. Biol Reprod, 2013. **89**(2): p. 31.
27. Lim, H., et al., *Multiple female reproductive failures in cyclooxygenase 2-deficient mice*. Cell, 1997. **91**(2): p. 197-208.
28. Xiao, S., et al., *Differential gene expression profiling of mouse uterine luminal epithelium during periimplantation*. Reprod Sci, 2014. **21**(3): p. 351-62.
29. Rivera-Lopez, C.M., A.L. Tucker, and K.R. Lynch, *Lysophosphatidic acid (LPA) and angiogenesis*. Angiogenesis, 2008. **11**(3): p. 301-10.
30. Pereira, R.D., et al., *Angiogenesis in the placenta: the role of reactive oxygen species signaling*. Biomed Res Int, 2015. **2015**: p. 814543.
31. Li, Q., et al., *The antiproliferative action of progesterone in uterine epithelium is mediated by Hand2*. Science, 2011. **331**(6019): p. 912-6.

32. Diao, H., et al., *Temporal expression pattern of progesterone receptor in the uterine luminal epithelium suggests its requirement during early events of implantation*. *Fertil Steril*, 2011. **95**(6): p. 2087-93.
33. Li, R., et al., *Segregated responses of mammary gland development and vaginal opening to prepubertal genistein exposure in Bcl2(-/-) female mice with lipodystrophy*. *Reprod Toxicol*, 2015. **54**: p. 76-83.
34. Li, R., et al., *Olfactomedin 1 Deficiency Leads to Defective Olfaction and Impaired Female Fertility*. *Endocrinology*, 2015. **156**(9): p. 3344-57.